Virology 414 (2011) 1–9

Contents lists available at ScienceDirect

Virology

journal homepage: www.elsevier.com/locate/yviro

Rapid Communication

In vivo analysis of the cell cycle dependent association of the bovine papillomavirus E2 protein and ChlR1

Katherine M. Feeney, Anastasia Saade [1], Krzysztof Okrasa, Joanna L. Parish *

School of Medicine, University of St Andrews, Medical and Biological Sciences Building, North Haugh, St Andrews, Fife, KY16 9TF, UK

ARTICLE INFO

Article history:
Received 1 December 2010
Returned to author for revision
14 January 2011
Accepted 17 March 2011
Available online 13 April 2011

Keywords:
Papillomavirus
Segregation
Mitosis
Helicase
FRET

ABSTRACT

It has been shown that the genomes of episomally maintained DNA viruses are tethered to host cell chromosomes during cell division, facilitating maintenance in dividing cells. The papillomavirus E2 protein serves this mechanism of viral genome persistence by simultaneously associating with chromatin and the viral genome during mitosis. Several host cell proteins are reported to be necessary for the association of E2 with chromatin including the cohesion establishment factor ChlR1. Here we use fluorescence resonance energy transfer (FRET) technology to confirm the interaction between BPV-1 E2 and ChlR1. Furthermore, we use synchronised live cells to study the temporal nature of this dynamic protein interaction and show that ChlR1 and E2 interact during specific phases of the cell cycle. These data provide evidence that the association of E2 with ChlR1 contributes to a loading mechanism during DNA replication rather than direct tethering during mitotic division.

Introduction

Human papillomaviruses (HPVs) are the aetiological agents of benign and malignant lesions of differentiating cutaneous and mucosal squamous epithelium. Infection with high risk HPV types, for example HPV-16 and HPV-18, is linked to the progression of the majority of cervical cancers, in addition to a substantial subset of other anogenital and head and neck carcinomas (zur Hausen, 2009). Approximately 100 HPV types have been isolated, each classified depending on their infection site preference and clinical outcome (de Villiers et al., 2004).

The PV life cycle is intimately linked to the differentiation of epithelial cells. Infection is established in the basal cells of the epithelium where the genome is maintained as an extra-chromosomal episome that replicates along with the cellular DNA during S phase (Kadaja et al., 2009). Viral replication requires the viral E1 and E2 proteins, which together melt the origin of replication and recruit cellular proteins required for replication such as replication protein A and DNA polymerase α primase (Conger et al., 1999; Han et al., 1999; Loo and Melendy, 2004; Masterson et al., 1998). E2 functions in the transcriptional regulation of early gene expression (Gloss and Bernard, 1990; Spalholz et al., 1988). As infected cells differentiate, they migrate away from the basal layer and into the upper layers of the epidermis. Late gene expression is then activated allowing expression of capsid proteins and assembly of infectious virions.

Throughout the viral life cycle, the approximately 8000 base pair PV genomes are stably maintained as autonomous, multi-copy circular double-stranded DNA plasmids. The PV genome does not encode a canonical centromeric region (Calos, 1998) and therefore cannot assemble kinetochore-like structures that could be used to facilitate genome segregation during mitosis. The segregation of episomal viral genomes into daughter cells is an obstacle that all low-copy number episomal viruses should overcome in order to maintain viral persistence (Feeney and Parish, 2009). The PV E2 protein serves this function by tethering PV episomes to mitotic chromosomes (Bastien and McBride, 2000; Skiadopoulos and McBride, 1998), although the specific mechanism remains unresolved.

The E2 protein encoded by all papillomavirus types is around 42 kDa in size and contains a C-terminal DNA binding and dimerisation domain and an N-terminal transactivation domain. These functional domains are linked by a flexible hinge region (Hegde, 2002). To facilitate viral genome tethering during mitosis, it is thought that the C-terminal DNA binding domain of E2 specifically binds to consensus sequences within the viral genome while associating with host cell chromosomes via its N-terminal domain (Bastien and McBride, 2000; Skiadopoulos and McBride, 1998). However, it has been shown that the dimerisation of E2, facilitated at the C-terminus of the protein, seems to be required for the efficient interaction of E2 with host cell chromosomes (Cardenas-Mora et al., 2008). The N-terminal domain of E2 does not itself directly bind to DNA and as such E2 targets host cell chromatin associated protein(s) to facilitate tethering. Several host cell proteins have been reported to act as a chromatin receptor for E2 during mitosis.

* Corresponding author. Fax: +44 1334 463482.
E-mail address: jlp10@st-andrews.ac.uk (J.L. Parish).
[1] Present address: Goethe-University Frankfurt, Institute of Anatomy III, 60590 Frankfurt, Germany.

0042-6822/$ – see front matter © 2011 Elsevier Inc. All rights reserved.
doi:10.1016/j.virol.2011.03.015

The bromodomain family member, Brd4 was first identified as the chromatin binding receptor for E2 (You et al., 2004). Brd4 is a member of the BET family of transcriptional regulators and binds to DNA by interacting with acetylated H3 and H4 histones through its two bromodomains (Dey et al., 2003). Brd4 has been shown to diffusely coat the surface of mitotic chromosomes and expression of E2 results in recruitment of Brd4 to punctate foci that co-localise with E2 throughout mitosis (Abbate et al., 2006; McPhillips et al., 2005; You et al., 2004). In addition, the over-expression of the C-terminal domain of Brd4 that contains the E2 binding site results in a loss of viral genomes. Interestingly, it has been demonstrated that Brd4 interaction is also important for E2-dependent transcription regulation and viral genome replication, suggesting that this interaction plays an important role in multiple processes in the viral life cycle (Ilves et al., 2006; Schweiger et al., 2006; Senechal et al., 2007; Wu and Chiang, 2007; Wu et al., 2006). In addition, it has been demonstrated that association of E2 with Brd4 is not required for genome partitioning of all papillomavirus types (McPhillips et al., 2006) and that depletion of Brd4 has no effect on the association of E2 with mitotic chromosomes (Parish et al., 2006a). Put together these data suggest a role for Brd4 in viral genome tethering, but that Brd4 interaction may not be essential for this important process.

A second cellular protein implicated in the E2-dependent tethering of viral genomes during mitosis is the topoisomerase binding protein TopBP1. An interaction between HPV-16 E2 and TopBP1 was identified (Boner et al., 2002) and TopBP1 was subsequently shown to regulate the affinity of E2 with cellular chromatin. Furthermore E2 and TopBP1 co-localise on mitotic chromosomes at late stages of mitosis, further substantiating the hypothesis that TopBP1 plays a role in E2-mediated viral genome tethering. In addition to these studies, we have isolated the DNA helicase, ChlR1 as a cellular binding protein of E2 (Parish et al., 2006a). ChlR1 plays a role in sister chromatid cohesion establishment and as such is important in the accurate segregation of cellular chromosomes during mitosis (Inoue et al., 2007; Parish et al., 2006b). In order to define the role of ChlR1 interaction in the viral life cycle, we isolated a mutant of BPV-1 E2 (W130R) that fails to associate with ChlR1. E2 W130R retains important functions to wild type levels such as transcriptional activation and viral genome replication. In addition, E2 W130R associates with known binding partners of E2 such as E1, Brd4, Gps2 (Breiding et al., 1997; Grossel et al., 1996; Parish et al., 2006a) and TopBP1 (Parish, unpublished). Using E2 W130R, we determined that ChlR1 interaction was required for the association of E2 with chromosomes and stable genome maintenance in dividing cells. To confirm these data we used RNA interference to deplete endogenous ChlR1 protein, which resulted in an abrogation of the association of E2 with mitotic chromosomes. These studies demonstrate that interaction with ChlR1 is required for viral genome tethering to mitotic chromosomes. However, we hypothesise that ChlR1 itself is not the mitotic tether for E2 since these two proteins do not co-localise on mitotic chromosomes; ChlR1 associates with chromosomes during the very early stages of mitosis only. These observations strongly suggest that ChlR1 is required for the loading of E2-associated viral genomes onto chromosomes during DNA replication at S-phase, but not for their retention during mitosis. To confirm this hypothesis, we have used co-immunoprecipitation assays and fluorescence resonance energy transfer (FRET) technology in live cells synchronised at specific stages of the cell cycle to analyse the temporal nature of the interaction between ChlR1 and BPV-1 E2.

Results

Characterisation of BPV-1 E2 and ChlR1 fusion proteins

The bovine papillomavirus type 1 (BPV-1) E2 protein has been shown to co-localise with endogenous ChlR1 protein in the nucleus, with nucleolar exclusion in the African green monkey kidney CV-1 cell line (Parish et al. 2006a). Here, hTERT immortalised retinal pigment epithelial cells (hTERT-RPE1) were used to assess the interaction between ChlR1–YFP and E2–CFP fusion proteins. hTERT-RPE1 cells were used throughout the present study for several reasons. Firstly, they are a human epithelial cell line and are therefore similar in origin to other cell lines that have historically been used to study papillomavirus protein function. In addition, hTERT-RPE1 cells are functionally and phenotypically normal and are arrested by serum deprivation, contact inhibition and cell cycle inhibitors such as thymidine and nocodazole (Jiang et al. 1999). Therefore tight cell cycle synchronisation of these cells can be achieved, allowing the study of cell cycle dependent protein interactions. To assess the expression and localisation of ChlR1–YFP and E2–CFP in hTERT-RPE1 cells, cells were co-transfected and the subcellular localisation of each fusion protein assessed by direct fluorescence using confocal microscopy (Fig. 1A). E2–CFP and ChlR1–YFP are localised to the nuclear compartment with nucleolar exclusion as previously described for the native proteins, showing that the fluorescent tags do not affect protein targeting to the nuclear compartment. Some cytoplasmic expression was visible in cells expressing higher amounts of the fusion proteins. In addition, an E2 protein containing a point mutant at position tryptophan 130 (W130R), previously shown to be unable to bind to ChlR1 while retaining wild type transcription activation and replication functions of E2 (Breiding et al., 1997; Grossel et al., 1996; Parish et al., 2006a), was expressed as a CFP fusion protein (E2W130R–CFP). Like E2–CFP, E2W130R–CFP co-localised with ChlR1–YFP in the nucleus of co-transfected cells with nucleolar exclusion. To ensure that the fusion proteins were correctly expressed, Western blot analysis using B201 and ChlR1 antibodies respectively confirmed that the E2–CFP, E2W130R–CFP and ChlR1–YFP fusion proteins are the appropriate size (Figs. 1C, 3 and 5B).

To provide evidence that the E2 fusion proteins used in this study are able to bind DNA and retain wild type E2 transactivation activity, the ability of E2–CFP to activate transcription from a synthetic Luciferase reporter plasmid was compared to wild type E2 protein. hTERT-RPE1 cells were transfected with reporter alone or in combination with increasing amounts of E2 expression plasmid. The data in Fig. 1B and C clearly show that E2–CFP is able to activate transcription in a dose responsive manner to levels comparable to wild type E2 protein, indicating that the transcription activation function of E2 is not impaired by the addition of the C-terminal fluorescent protein tag. Like E2–CFP, E2W130R–CFP is also able to activate transcription in a dose responsive manner to levels similar to wild type E2 (Fig. 1B).

We have previously shown that ChlR1 functions in the establishment of sister chromatid cohesion and that depletion of ChlR1 from HeLa cells results in abnormal sister chromatid cohesion (Parish et al, 2006b). To provide evidence that the ChlR1–YFP fusion protein used in this study is active and like native ChlR1, functions in the cohesion establishment pathway, hTERT-RPE1 cells were transfected a siRNA oligonucleotide that targets the 3′UTR of ChlR1 to deplete cells of endogenous ChlR1 protein, or a non-targeting siRNA oligonucleotide as a negative control. In parallel, cells were co-transfected with ChlR1 siRNA and ChlR1–YFP expression plasmid, which is insensitive to the 3′UTR specific ChlR1 siRNA. Cells were then blocked with nocodazole for 3 h before harvesting for Western blot analysis and metaphase spread analysis to assess sister chromatid cohesion. Transfection of cells with ChlR1-specific siRNA resulted in efficient depletion of ChlR1 protein as compared to untransfected cells or cells transfected with non-targeting siRNA. Co-transfection of cells with ChlR1 siRNA and ChlR1–YFP expression plasmid resulted in depletion of endogenous ChlR1 protein in conjunction with co-expression of exogenous ChlR1–YFP (Fig. 2A) with approximately 70% of cells expressing ChlR1–YFP (data not shown). Analysis of metaphase spreads generated from the same transfected cell populations revealed that while cells transfected with non-targeting control siRNA showed normal sister chromatid cohesion, cells with depleted ChlR1 protein had significantly fewer metaphase cells, presumably because hTERT-RPE1 cells will arrest at the G2

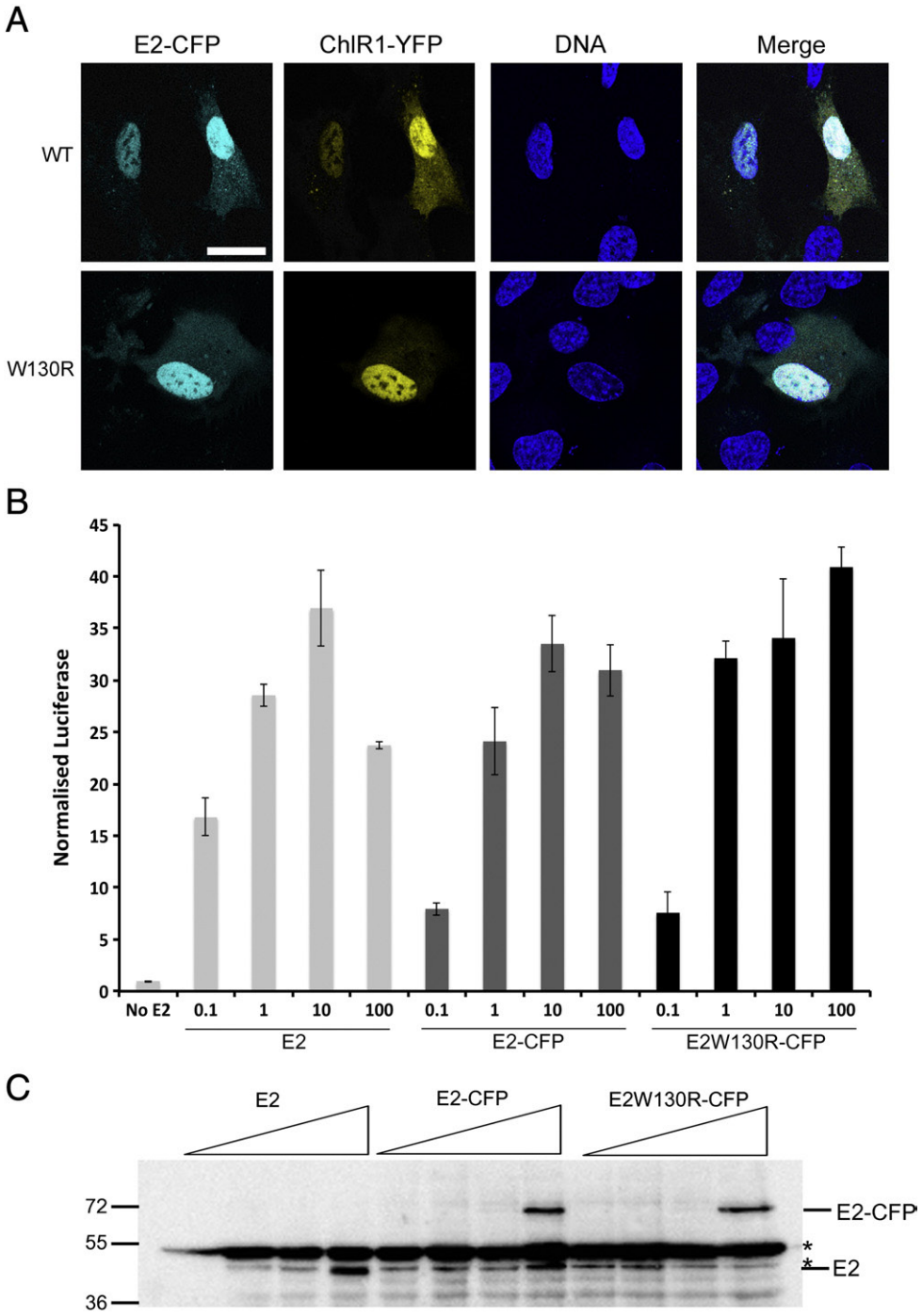

Fig. 1. Functional analysis of E2–CFP and ChlR1–YFP fusions. hTERT-RPE1 cells were co-transfected with pcDNA–E2–CFP and pcDNA–ChlR1–YFP and subcellular localisation of the expressed proteins was assessed by fluorescent confocal microscopy. E2–CFP (cyan) and ChlR1–CFP (yellow) co-localise in the nuclear compartment with nucleolar exclusion as assessed by staining DNA with Hoechst 33342 (blue). Scale bar indicates 20 μm. (B) hTERT-RPE1 cells were co-transfected with 10 ng *Renilla* Luciferase, 100 ng of the E2 responsive firefly Luciferase reporter, 6E2-tk-Luc, and 0.1, 1, 10 or 100 ng of E2, E2–CFP or E2W130R–CFP expression plasmid. Luciferase activity was determined as described in Materials and methods. The recorded firefly Luciferase activity was normalised to the *Renilla* activity and the data shown represents the mean and standard deviation of three independent experiments. (C) Cell lysates taken from the transcription assay described in (B) were separated by SDS-PAGE and the expression of E2 protein detected by Western blot using B201 (obtained from E. Androphy, Indiana University). E2 and E2–CFP fusions proteins are indicated along with non-specific spurious bands (*), one of which runs immediately above the native E2 protein (visible in lane 4). Molecular weight standards are indicated on the left.

checkpoint if genome integrity is lost. Nonetheless, the majority of the metaphase spreads in the ChlR1 depleted sample displayed abnormal sister chromatid cohesion (7 out of 9). In contrast, cells co-transfected with ChlR1 siRNA to deplete endogenous ChlR1 protein and ChlR1–YFP expression plasmid showed normal sister chromatid cohesion in the majority of metaphase spreads analysed (16 out of 19). Representative images are shown in Fig. 2B. These data indicate that the ChlR1–YFP protein is able to functionally replace endogenous ChlR1.

ChlR1 and E2 fusion proteins associate in vivo

After ensuring that E2 and ChlR1 fusion proteins were correctly expressed, localised and retained wild type activity, an immunoprecipitation assay was performed to confirm the interaction between ChlR1 and E2 fusion proteins. hTERT-RPE1 cells were co-transfected with combinations of plasmids expressing C-terminally tagged ChlR1 and E2 proteins. Whole cell lysates were immunoprecipitated with E2 specific

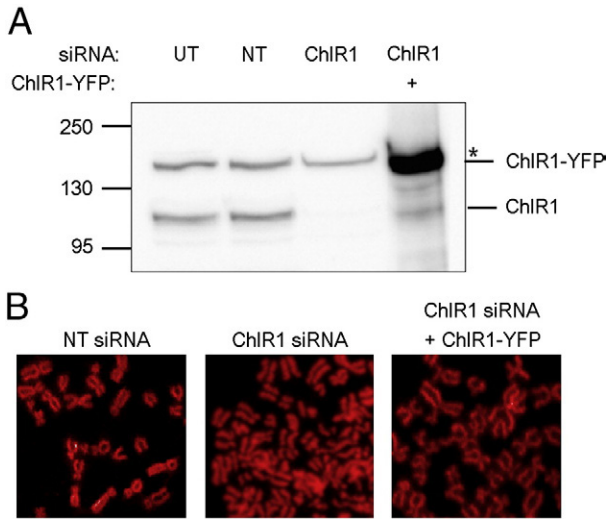

Fig. 2. Functional analysis of ChlR1–YFP. hTERT-RPE1 cells were transfected with non-targeting control siRNA (NT) or siRNA specific to the 3′ UTR of ChlR1. Cells transfected with ChlR1 siRNA were also co-transfected with ChlR1–YFP expressing plasmid. (A) The expression of endogenous ChlR1 and ChlR1–YFP was compared to untransfected cells (UT) by Western blot. Protein concentration of whole lysates was determined by BCA assay (Pierce) and 30 μg total protein was separated by SDS-PAGE prior to Western blotting using anti-ChlR1 antibody. Endogenous ChlR1 and ChlR1–YFP proteins are indicated along with a spurious band (*), which runs close to the molecular weight of ChlR1–YFP. Molecular weight standards are indicated on the left. (B) Metaphase chromosome morphology was determined in each cell population by metaphase spread. DNA was stained with propidium iodide and chromosomes visualised by confocal microscopy.

antibody B201, and the presence of co-precipitating ChlR1 protein was detected by Western blot (Fig. 3). Co-immunoprecipitation of ChlR1–YFP with E2–CFP was confirmed, providing evidence that the C-terminal fluorescent protein tag does not disrupt the interaction between E2 and ChlR1. Conversely, co-immunoprecipitation of ChlR1–YFP with E2–CFP was not observed when cell lysates were incubated with an irrelevant antibody (FLAG), and ChlR1–YFP was not immunoprecipitated with E2 antibody from cells transfected with ChlR1–YFP alone. To further validate the specificity of the interaction between E2–CFP and ChlR1–YFP, cells were co-transfected with ChlR1–CFP and E2W130R–YFP. While the E2W130R–CFP protein was efficiently immunoprecipitated with B201 antibody, co-precipitating ChlR1–YFP was not detected, providing evidence that the fluorescent tags associated with these proteins do not facilitate non-specific interactions between E2 and ChlR1.

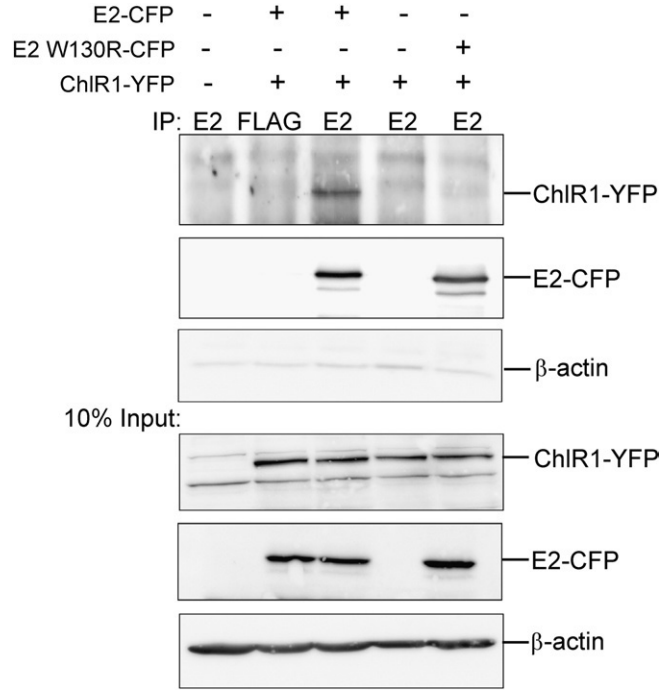

Fig. 3. Co-immunoprecipitation of E2 and ChlR1 fusion proteins. hTERT-RPE1 cells were co-transfected with constructs expressing E2–CFP and ChlR1–YFP, ChlR1–YFP alone or E2W130R–CFP and ChlR1–YFP as shown. Whole cell extracts were immunoprecipitated with E2 specific antibody B201 or non-specific FLAG antibody and the presence of co-precipitating ChlR1 detected on the same membrane by western blot. The membrane was then stripped and re-probed with β-actin antibody. The lower three panels show 10% input of the E2 and ChlR1 proteins for each co-immunoprecipitation reaction and β-actin loading control.

Characterisation of ChlR1 and E2 interaction in vivo using FRET

FRET is used to study protein–protein interactions and takes advantage of a direct energy transfer between two closely associated fluorophores. In order for FRET to occur, proteins need to be within 10 nm of each other and therefore likely to be directly associated (Piston and Kremers, 2007). To determine if E2 and ChlR1 are closely associated, FRET efficiency between the CFP and the YFP moieties was measured using confocal microscopy and the acceptor photobleaching method. To validate our results, we used two negative and two positive controls. Linked CFP–YFP fusion constructs, pCYa and pCYx were used as positive controls. The donor alone (E2–CFP) and the donor with free YFP were used as negative controls as no transfer of energy occurs in the absence of the acceptor and between the donor and the empty pYFP-C1 plasmid.

To determine the FRET efficiency between E2–CFP and ChlR1–YFP, we examined individual regions of interest (ROIs) throughout the cell and found that a positive FRET signal was only observed in the nuclear compartment regardless of whether cytoplasmic staining of the fluorescent proteins was visible (data not shown). Therefore, for the remainder of the FRET experiments described in this manuscript ROIs within the nuclear compartment of co-transfected cells only were chosen. As expected, a positive FRET efficiency was observed in cells expressing $CFP(x)_7YFP$ and $CFP(x)_{15}YFP$ fusion proteins from constructs pCYx and pCYa respectively and little or no FRET was observed when cells were transfected with E2–CFP alone or E2–CFP and native YFP (Fig. 4). Interestingly, cells expressing E2–CFP and ChlR1–YFP displayed a positive average FRET efficiency of 16.05%, significantly higher than that observed with the negative controls and with a similar FRET efficiency as that recorded between the CFP–YFP fusions used as a positive control. Since FRET efficiency reduces as the distance between the acceptor and the donor increases (Kenworthy, 2001), these data

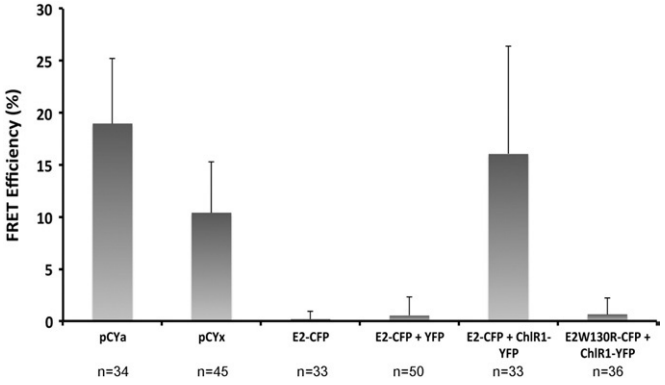

Fig. 4. Measurement of FRET between E2–CFP and ChlR1–YFP. hTERT-RPE1 cells were transfected with plasmids expressing proteins as indicated on the x axis. FRET efficiency was assessed using acceptor photobleaching method as described in the materials and methods. The data shown represent the mean and standard deviation of 4 ROIs taken from at least 33 individual cells (the number of cells (*n*) assayed in each data point is indicated).

provide strong evidence that E2 and ChlR1 are in close molecular proximity within the nuclear compartment. However, the large standard deviation (±10.32%) within this data set suggests that either the FRET signals in the nucleus are dependent on specific localisation or that the association of E2 with ChlR1 depends on the physical state of individual cells.

To further validate the positive FRET efficiency observed between E2–CFP and ChlR1–YFP, cells were co-transfected with E2W130R–CFP and ChlR1–YFP expressing plasmids. While both fusion proteins were efficiently expressed in the analysed cells, only a very low FRET efficiency between these two molecules was recorded (Fig. 4), providing strong evidence that the positive FRET signal observed between wild type E2–CFP and ChlR1–YFP is directly due to an interaction between E2 and ChlR1 and not due to non-specific fluorescent energy transfer between CFP and YFP molecules that are localised to the same cellular compartment.

FRET efficiency between ChlR1 and E2 fusion proteins is dynamic throughout the cell cycle

To determine the dynamic nature of the interaction between E2 and ChlR1 throughout the cell cycle, we performed FRET analysis on cells which were arrested in G1 by serum starvation, early-S phase by thymidine block, mid-S phase by thymidine block followed by a 3-h release and in mitosis by incubation with nocodazole. The synchrony of the cell populations was determined by flow cytometry of propidium iodide stained cells (Fig. 5A). To ensure that the fusion proteins were expressed in all synchronised populations at levels comparable to those observed in asynchronously growing cells, E2–CFP and ChlR1–YFP expression levels were determined by Western blot (Fig. 5B). While a small reduction in the expression of E2–CFP and ChlR1–YFP was observed in cells arrested in G1, the expression of both fusion proteins was comparable in cells arrested at early S phase, actively replicating DNA in mid-S phase, or in mitosis. Measurement of the FRET efficiency between E2–CFP and ChlR1–YFP in cells arrested in G1 by serum starvation revealed a positive FRET efficiency of 10.42 ± 5.12% (Fig. 5C). This FRET efficiency was maintained into S phase (9.32 ± 4.41%) and interestingly was significantly increased as cells progressed into mid-S phase (26.73% ± 7.29, $p = 1.36 \times 10^{-12}$). In contrast, cells arrested in mitosis showed a very low FRET efficiency of 1.2 ± 1.62% which is close to the efficiency observed in the unbleached negative control (0.76 ± 1.46%) and reflective of the loss of co-localisation of the fusion proteins as cells enter mitosis (Fig. 5D). This confirms our earlier observation that E2 and ChlR1 do not co-localise on chromosomes during mitosis (Parish et al., 2006a).

To confirm these data and determine whether native E2 protein associates with endogenous ChlR1 protein in a cell cycle dependent manner, hTERT-RPE1 cells were transfected with an E2 expressing plasmid. Twenty-four hours following transfection, cells were removed from the tissue culture dish, pooled and reseeded to fresh 6 cm dishes. Cells were then arrested in G1 by serum starvation, S phase by thymidine block, mid-S phase by thymidine block followed by a 3- and 5-h release and in mitosis by incubation with nocodazole. Cells were harvested and the association of E2 with endogenous ChlR1 determined by co-immunoprecipitation with ChlR1 specific antibody. The data in Fig. 6 show that while endogenous ChlR1 protein levels are similar in all cell populations, E2 protein is stabilised somewhat in cells arrested in early S phase, as previously demonstrated (Johansson et al, 2009). In agreement with the FRET data shown in Fig. 5, immunoprecipitation with ChlR1 specific antibody in lysates from synchronised cells shows that E2 associates with endogenous ChlR1 with the highest affinity during mid-S phase (Fig. 6), thus providing evidence that the strong FRET signal between E2–CFP with ChlR1–YFP during mid-S phase does indeed reflect an increase in the association of native E2 protein with ChlR1.

Discussion

The data presented in this study provide strong evidence that E2 and ChlR1 directly associate *in vivo* and novel insight into the dynamic and temporal nature of this interaction. ChlR1 and E2 proteins were fused to YFP and CFP respectively. Correct expression, sub-cellular localisation and function of the fusion proteins were confirmed (Figs. 1 and 2) and association of the recombinant proteins assayed by co-immunoprecipitation (Fig. 3). Based on these data E2–CFP and ChlR1–YFP were used in subsequent FRET experiments. The measurement of the FRET efficiency between this protein pair revealed a robust and significant protein–protein interaction that was dramatically reduced to levels observed with negative controls when the E2 mutant W130R CFP fusion was co-transfected with ChlR1–CFP. The loss of FRET between E2W130R–CFP and ChlR1–YFP confirms firstly that this mutation disrupts that association of E2 with ChlR1 and also that the FRET signal observed between E2–CFP and ChlR1–YFP is due to specific association of E2 and ChlR1 and not aggregation of the exogenously expressed fusion proteins. The FRET efficiency between E2–CFP and ChlR1–YFP was surprisingly high and in line with that observed with the positive controls. In addition, the heterogeneous FRET efficiencies from cell to cell transfected with E2–CFP and ChlR1–CFP reflected a large degree of variation in the efficiency of FRET between E2 and ChlR1 in a mixed cell population, and led to the hypothesis that the interaction between E2 and ChlR1 was dependent on the specific cell cycle phase.

In order to test this hypothesis, cells were arrested in G1, early and mid-S phase and mitosis, and the interaction between ChlR1 and E2 measured. A robust and significant FRET efficiency between ChlR1–YFP and E2–CFP was observed in G1 and early S phase, which dramatically increased as cells progressed into mid-S phase (Fig. 5). Interestingly no association of E2–CFP and ChlR1–YFP was detected in cells arrested in mitosis. These data are confirmed by co-immunoprecipitation of E2 protein with endogenous ChlR1 in cells synchronised in early and mid-S phase, with minimal association detected in cells synchronised in G1 phase, late-S phase or mitosis (Fig. 6).

We have previously shown that E2 interacts with ChlR1 in order to facilitate viral genome segregation during mitosis (Parish et al., 2006a) but whether ChlR1 interaction is required for physically tethering viral genomes onto mitotic chromosomes or for loading genomes onto chromatin prior to mitotic segregation was unresolved. Co-localisation data suggested the latter scenario since E2 and ChlR1 co-localise as chromosomes begin to condense, but not when cells enter mitosis. The data presented here show that ChlR1 and E2 only associate during G1 and S phase of the cell cycle and while the interaction with ChlR1 is important for viral genome tethering, interaction with other cellular proteins must be required for the physical association of E2 with host cell chromosomes during mitosis. Several candidate proteins involved in papillomavirus genome segregation have been described including Brd4 and TopBP1. It will be interesting to study the dynamics of these protein interactions in live cells in order to determine their importance in the segregation of viral DNA.

Several studies in budding yeast have shown that the ChlR1 homologue Chl1 associates with components of the cellular replication machinery including replication factor C (RFC) and proliferating cell nuclear antigen (PCNA) (Mayer et al., 2004; Moldovan et al., 2006; Petronczki et al., 2004), and interaction with the RFC complex stimulates ChlR1 helicase activity (Farina et al., 2008). Depletion or mutation of ChlR1 or the yeast homologue results in inefficient sister chromatid cohesion and defects in chromosome segregation (Gerring et al., 1990; Inoue et al., 2007; Parish et al., 2006b; Skibbens, 2004). In addition, ChlR1 physically associates with the cohesin complex (Inoue et al., 2007; Parish et al., 2006b). Putting these data together it is thought that ChlR1 function is required for sister chromatid cohesion establishment during DNA replication. Interestingly, ChlR1 also associates with the flap

endonuclease Fen1 and Fen1 activity is stimulated by ChlR1, suggesting that ChlR1 may play a role in the processing of lagging strands during cohesion establishment (Farina et al., 2008).

The recruitment of E2 and bound viral genomes to host cell chromosomes must presumably occur before entry into mitosis. In order to facilitate this, E2 targets the cohesion establishment pathway

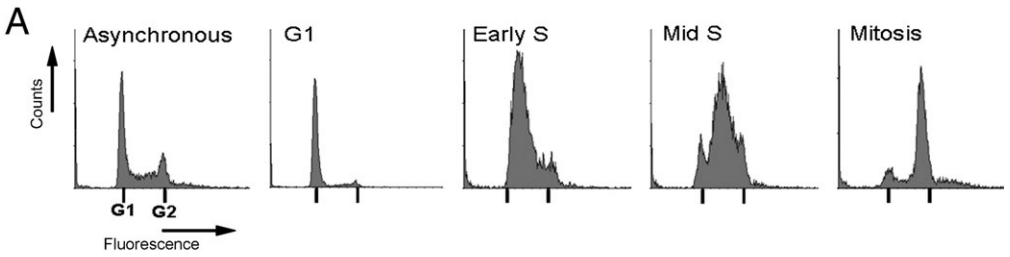

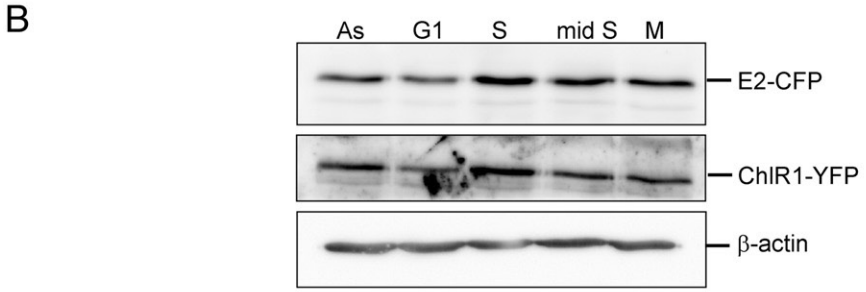

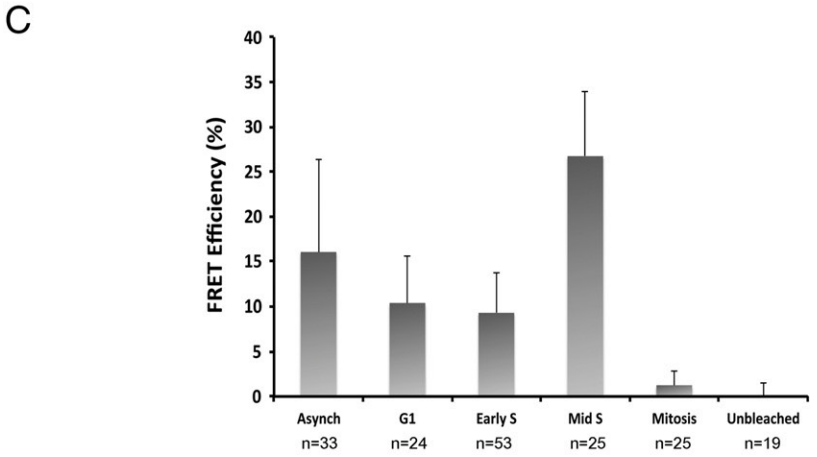

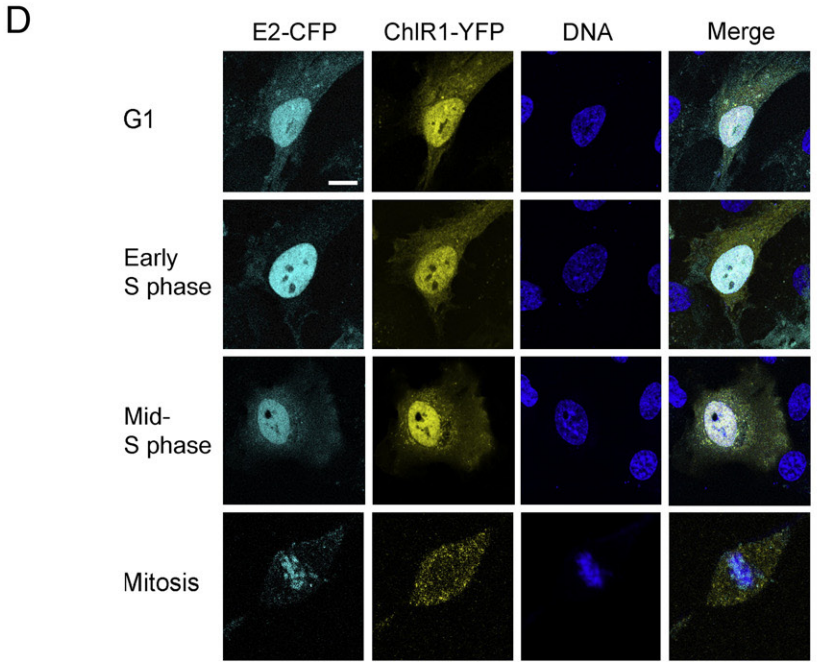

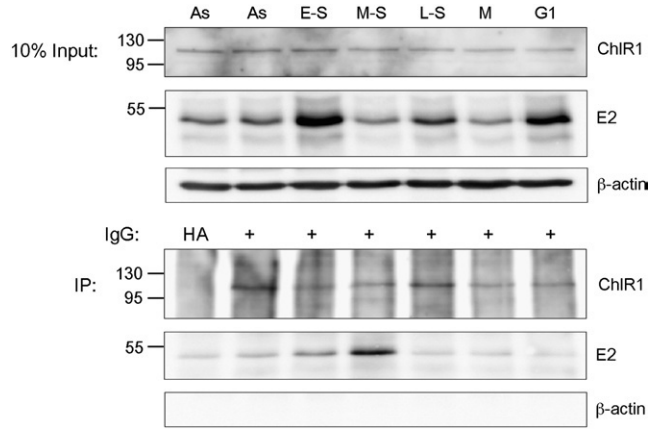

Fig. 6. Cell cycle dependent association of BPV-1 E2 and endogenous ChlR1. hTERT-RPE1 cells were transfected with E2 expressing plasmid. Twenty-four hours following transfection, cells were trypsinised, pooled and reseeded into fresh tissue culture dishes at approximately 30% of their original density. Cells were then arrested in early-S phase (E-S) by thymidine block or released from the thymidine block and harvested in mid-S phase 3 h post release (M-S) or in late S phase 5 h post release (L-S). Cells were also arrested in G1 by serum starvation or in mitosis (M) by incubation in nocodazole. Ten percent input of the whole cell extracts used for co-immunoprecipitation experiments is shown in the top two panels indicating ChlR1 and E2 expression, respectively. Lysates were immunoprecipitated with either HA (12CA5) antibody as a negative control or ChlR1 specific antibody and immunoprecipitated ChlR1 protein on the upper half of the membrane is shown. The presence of co-precipitating E2 protein, detected with B201 antibody is shown in the lower panel. The lower half of each membrane was stripped and re-probed with β-actin antibody to show equal loading and specificity of protein co-immunoprecipitation.

via its association with ChlR1 and ensures that viral genomes are tethered to chromosomes as the replication fork progresses during S phase. Association between ChlR1 and E2 is then disrupted but E2 remains tethered to chromosomes via interaction with another cellular protein or protein(s). Elucidation of this intriguing mechanism of passing viral episomes to daughter cells and ensuring nuclear retention will not only help in the understanding of host cell chromosome segregation but also provide a useful clinical target in the design of novel antiviral therapeutics.

Materials and methods

Cell culture

hTERT-immortalised human retinal pigment epithelial cells (hTERT-RPE1) were maintained in 50% Dulbecco's Eagle's Modified Medium and 50% F-12 (DMEM/F-12) supplemented with 10% foetal bovine serum. Cells were transfected using Fugene DH (Roche) at a DNA/Fugene ratio of 1:3. For synchronization, cells were treated with serum-free medium, 2 mM thymidine or 100 ng/ml nocodazole for 16 h. For thymidine release experiments, cells were washed three times with 37 °C PBS and fresh 37 °C medium added. Cells were then harvested 3 h post release to obtain a population of cells synchronised in mid-S phase.

Constructs

pcDNA3-ChlR1–CFP expresses human ChlR1 fused to CFP at the C-terminal end of ChlR1. pcDNA3–E2–YFP expresses BPV-1 E2 fused to YFP at the C-terminal end of E2. pcDNA3–E2W130R–YFP expresses BPV-1 E2 W130R fused to YFP at the C-terminal end of E2. pEYFP-C1 (Clontech) expresses YFP. pCYx and pCYa (obtained from Dr. Laura Trinkle-Mulcahy, College of Life Sciences, University of Dundee) express CFP fused to YFP with 7 and 15 amino acid spacers respectively and were used as positive controls for FRET experiments. pRL-CMV (Promega) constiutively expresses *Renilla* luciferase and p6E2-tk-Luc (obtained from Professor Iain Morgan, University of Glasgow) contains 6 E2 binding sites upstream of the gene encoding firefly Luciferase.

Antibodies

The N-terminal 1–130 amino acids of ChlR1 were cloned into pET24b using NdeI and XhoI restriction sites. The resulting pET24b-130-ChlR1 expresses ChlR1 1–130 with a hexahistidine tag at the C-terminus (LEHHHHHH). pET24b-130-CHlR1 was transformed into Rosetta(DE3)2 pLyS *Escherichia coli* (Novagen) and expressed at 30 °C for 3–4 h after induction with 0.5 mM IPTG. Cells were harvested and pellets resuspended in lysis buffer (20 mM Tris–HCl, pH 8.0, 250 mM NaCl). Lysis was performed at room temperature using lysosyme (Sigma), followed by a 20-s sonication at 4 °C, 70% amplitude. The lysate was then cleared by centrifugation at 10,000*g* for 15 min at 4 °C and the supernatant loaded onto a HiTrap-Chelating HP column charged with Ni^{2+} (GE Healthcare). After washing with 10 column volumes of wash buffer (phosphate buffer pH 7.4, 500 mM NaCl, 60 mM imidazole), the purified protein was eluted with the same buffer containing 250 mM imidazole. Protein purity was assessed by SDS-PAGE and concentration determined by BCA assay. Protein was stored at 4 °C in 20 mM Tris–HCl buffer pH 8.0, 100 mM NaCl, 1 mM DTT. On average 26 mg of protein with 98% of purity was obtained from 500 ml of bacterial culture. Antibodies to ChlR1 1–130 were raised in rabbits by Dundee Cell Products and affinity purified on protein G sepharose resin.

B201 antibody recognises BPV-1 E2 (provided by Elliot Androphy, University of Indiana, USA). FLAG and β-actin antibodies were purchased from Sigma. Secondary horseradish peroxidase conjugated anti-mouse and anti-rabbit antibodies (Jackson ImmunoResearch) were detected using Supersignal West Dura (Pierce).

Transcription assays

hTERT-RPE1 cells were seeded into 6 well plates at a density of 1×10^5 and co-transfected with 10 ng pRL-CMV, 100 ng p6E2-tk-Luc and 0.1, 1, 10 or 100 ng of E2 expression plasmid. The amount of DNA in each transfection was normalised to 250 ng with salmon sperm DNA. Cells were harvested 24 h following transfection and lysed in 100 μl passive lysis buffer (Promega). Luciferase activity was measured in a 96 well Fluorostar Optima luminometer (BMG Labtech) using a Dual Luciferase assay kit (Promega) following the manufacturer's instructions. Each experiment was performed in triplicate.

RNA interference

hTERT-RPE1 cells were seeded into 60 mm tissue culture dishes at a density of 200,000 cells per dish in antibiotic free growth medium. Five hours later, cells were transfected with 100 nM non-targeting siRNA (iGENOME Non-Targeting siRNA #2, Thermo Fisher Scientific)

Fig. 5. Measurement of the association of E2 and ChlR1 at specific stages of the cell cycle. (A) The synchrony of hTERT-RPE1 cells expressing ChlR1–CFP and E2–YFP following G1 arrest by serum starvation, synchronisation in early and mid S phase arrest by thymidine block or nocodazole-induced mitotic arrest was determined by flow cytometry and compared to asynchronous population. (B) The expression level of E2–CFP and ChlR1–YFP in each cell population analysed was determined by western blot. Cells were synchronised as above and lysed. Equal amounts of protein from the whole cell extracts were separated by SDS-PAGE. The membrane was then probed with ChlR1, E2 and β-actin specific antibodies. (C) FRET efficiency of E2 and ChlR1 interaction in hTERT-RPE1 cells transfected and synchronised as in (A) was assessed using the acceptor photobleaching method as described in the materials and methods. The data shown represents the mean and standard deviation of 4 ROIs taken from at least 19 individual cells (the number of cells (n) assayed in each data point is indicated). (D) Subcellular localisation of the expressed proteins in synchronised cells was assessed by fluorescent confocal microscopy. E2–CFP (cyan) and ChlR1–CFP (yellow) co-localise in the nuclear compartment with nucleolar exclusion as assessed by co-staining the DNA with Hoechst 33342 (blue).

or ChlR1 3′ UTR specific siRNA (5′-AGUCACUCCUUCAGUAGAAUU-3′) using JetPRIME™ reagent, using 6 μl JetPRIME™ reagent per transfection and following the manufacturer's instructions (Polyplus Transfection Inc). Co-transfection with ChlR1–YFP expression plasmid was performed by adding 500 ng of pcDNA3–ChlR1–CFP to the transfection mix at the same time as adding the siRNA oligonucleotide. Cells were then incubated for 24 h.

Chromosomal spreads

siRNA transfected cells were blocked with 100 ng/ml nocodazole for 3 h and swelled in hypotonic buffer (0.8% sodium citrate) for 10 min at room temperature. Cells were fixed in Carnoy's fixative (75% methanol, 25% acetic acid) and spreads prepared by dropping suspended cells onto slides warmed to 37 °C. Slides were then stained with 1 mg/ml propidium iodide in PBS and mounted in Prolong Antifade (Invitrogen).

Co-immunoprecipitation assays

Cells were lysed for 30 min in freshly prepared lysis buffer (50 mM Tris–HCl 7.4, 100 mM NaCl, 20 mM NaF, 10 mM KH_2PO_4, 1% triton, 0.1 mM DTT, 10% glycerol and protease inhibitors (Sigma)). Cells were sonicated 2×10 s at 70% amplitude and cleared by centrifugation. For co-immunoprecipitation, 200 μl of lysate was mixed with 200 μl binding buffer (50 mM Tris–HCl 7.4, 100 mM KCl, 0.1 mM EDTA, 0.2% NP40, 0.1% BSA, 2.5% glycerol, 2 mM DTT and protease inhibitors), 10 μl of protein G sepharose (Sigma) and appropriate antibody. Samples were incubated at 4 °C for 2–3 h with gentle agitation followed by 3 washes with wash buffer (100 mM Tris–HCl 7.4, 100 mM NaCl, 0.5% NP40, 2 mM DTT and protease inhibitors). Co-immunoprecipitating proteins were separated by SDS-PAGE and detected by Western blot. Membranes were subsequently stripped and re-probed with β-actin antibody.

Fluorescence microscopy

Cells were cultured on coverslips. At 24 h post-transfection, cells were fixed in 4 % paraformaldehyde and nuclei stained with 5 μg/ml Hoechst 33342 (Molecular probes, Invitrogen) for 10 min. Coverslips were mounted on slides with Prolong Antifade (Invitrogen) and then sealed. Images were captured using a Leica TSC SP2 AOBS confocal laser scanning microscope.

FRET microscopy

FRET measurements were collected using the acceptor photobleaching method (Kenworthy, 2001). Cells were grown on glass bottomed dishes, coated with collagen (rat tail, type 1, Millipore) and were co-transfected with CFP and YFP fusion proteins at a 4:1 ratio. Images were captured using a Leica TSC SP2 AOBS confocal laser scanning microscope and a 63× oil immersion objective in a 37 °C chamber. The Krypton/Argon laser was set at 458 nm, 50% intensity to excite the CFP and at 514 nm, 50% and 100% intensity to excite and photobleach the YFP, respectively. CFP fluorescence was detected at 465–505 nm and YFP at 525–600 nm. Acceptor photobleaching was performed by stationary laser pulses of 150 ms at 514 nm, until 80% photobleaching was achieved. For all data points at least 7 individual cells were analysed with at least 4 regions of interest (ROIs) drawn in each.

Images were acquired using Leica acquisition and analysis software. Bleached regions, unbleached regions in the nucleus and regions outside the compartment of interest were selected to define background fluorescence. Because of the fast diffusion of unbleached acceptor molecules in the bleached regions, donor quenching was detected in a very short period of 1 s after photobleaching, acquiring post-bleaching images after 2 ms. FRET efficiency was calculated using the following formula:

$$\mathrm{FRET}_{\mathrm{eff}} = \left(\mathrm{D}_{\mathrm{post}} - \mathrm{D}_{\mathrm{pre}}\right) / \mathrm{D}_{\mathrm{post}}$$

Where D_{post} is the fluorescence intensity of the donor after acceptor photobleaching and D_{pre} is the fluorescence intensity of the donor before accepter photobleaching.

Flow cytometry

Cells were fixed with 5 ml of 70% ethanol, washed with PBS and labelled with 50 μg/ml propidium iodide containing 0.1 mg/ml RNase A in PBS for 30 min. Data were acquired using a FACScan flow cytometer (BD Biosciences) and analysed using Summit® v3.1 (DakoCytomation).

Acknowledgments

This work was funded by a Royal Society University Research Fellowship and a Medical Research Scotland project grant awarded to JLP.

References

Abbate, E.A., Voitenleitner, C., Botchan, M.R., 2006. Structure of the papillomavirus DNA-tethering complex E2:Brd4 and a peptide that ablates HPV chromosomal association. Mol. Cell 24 (6), 877–889.
Bastien, N., McBride, A.A., 2000. Interaction of the papillomavirus E2 protein with mitotic chromosomes. Virology 270 (1), 124–134.
Boner, W., Taylor, E.R., Tsirimonaki, E., Yamane, K., Campo, M.S., Morgan, I.M., 2002. A functional interaction between the human papillomavirus 16 transcription/replication factor E2 and the DNA damage response protein TopBP1. J. Biol. Chem. 277 (25), 22297–22303.
Breiding, D.E., Sverdrup, F., Grossel, M.J., Moscufo, N., Boonchai, W., Androphy, E.J., 1997. Functional interaction of a novel cellular protein with the papillomavirus E2 transactivation domain. Mol. Cell. Biol. 17 (12), 7208–7219.
Calos, M.P., 1998. Stability without a centromere. Proc. Natl Acad. Sci. U.S.A. 95 (8), 4084–4085.
Cardenas-Mora, J., Spindler, J.E., Jang, M.K., McBride, A.A., 2008. Dimerization of the papillomavirus E2 protein is required for efficient mitotic chromosome association and Brd4 binding. J. Virol. 82 (15), 7298–7305.
Conger, K.L., Liu, J.S., Kuo, S.R., Chow, L.T., Wang, T.S., 1999. Human papillomavirus DNA replication. Interactions between the viral E1 protein and two subunits of human DNA polymerase alpha/primase. J. Biol. Chem. 274 (5), 2696–2705.
de Villiers, E.M., Fauquet, C., Broker, T.R., Bernard, H.U., zur Hausen, H., 2004. Classification of papillomaviruses. Virology 324 (1), 17–27.
Dey, A., Chitsaz, F., Abbasi, A., Misteli, T., Ozato, K., 2003. The double bromodomain protein Brd4 binds to acetylated chromatin during interphase and mitosis. Proc. Natl Acad. Sci. U.S.A. 100 (15), 8758–8763.
Farina, A., Shin, J.H., Kim, D.H., Bermudez, V.P., Kelman, Z., Seo, Y.S., Hurwitz, J., 2008. Studies with the human cohesin establishment factor, ChlR1: association of ChlR1 with Ctf18-RFC and Fen1. J. Biol. Chem. 283 (30), 20925–20936.
Feeney, K.M., Parish, J.L., 2009. Targeting mitotic chromosomes: a conserved mechanism to ensure viral genome persistence. Proc. Biol. Sci. 276 (1662), 1535–1544.
Gerring, S.L., Spencer, F., Hieter, P., 1990. The CHL 1 (CTF 1) gene product of *Saccharomyces cerevisiae* is important for chromosome transmission and normal cell cycle progression in G2/M. EMBO J. 9 (13), 4347–4358.
Gloss, B., Bernard, H.U., 1990. The E6/E7 promoter of human papillomavirus type 16 is activated in the absence of E2 proteins by a sequence-aberrant Sp1 distal element. J. Virol. 64 (11), 5577–5584.
Grossel, M.J., Sverdrup, F., Breiding, D.E., Androphy, E.J., 1996. Transcriptional activation function is not required for stimulation of DNA replication by bovine papillomavirus type 1 E2. J. Virol. 70 (10), 7264–7269.
Han, Y., Loo, Y.M., Militello, K.T., Melendy, T., 1999. Interactions of the papovavirus DNA replication initiator proteins, bovine papillomavirus type 1 E1 and simian virus 40 large T antigen, with human replication protein A. J. Virol. 73 (6), 4899–4907.
Hegde, R.S., 2002. The papillomavirus E2 proteins: structure, function, and biology. Annu. Rev. Biophys. Biomol. Struct. 31, 343–360.
Ilves, I., Maemets, K., Silla, T., Janikson, K., Ustav, M., 2006. Brd4 is involved in multiple processes of the bovine papillomavirus type 1 life cycle. J. Virol. 80 (7), 3660–3665.
Inoue, A., Li, T., Roby, S.K., Valentine, M.B., Inoue, M., Boyd, K., Kidd, V.J., Lahti, J.M., 2007. Loss of ChlR1 helicase in mouse causes lethality due to the accumulation of aneuploid cells generated by cohesion defects and placental malformation. Cell Cycle 6 (13), 1646–1654.
Jiang, X.R., Jimenez, G., Frolkis, M., Kusler, B., Sage, M., Beeche, M., Bodnar, A.G., Wahl, G.M., Tlsty, T.D., Chiu, C.P., 1999. Telomerase expression in human somatic cells does not

induce changes associated with a transformed phenotype. Nat. Genet. 21 (1), 111–114.
Johansson, C., Graham, S.V., Dornan, E.S., Morgan, I.M., 2009. The human papillomavirus 16 E2 protein is stabilised in S phase. Virology 394 (2), 194–199.
Kadaja, M., Silla, T., Ustav, E., Ustav, M., 2009. Papillomavirus DNA replication—from initiation to genomic instability. Virology 384 (2), 360–368.
Kenworthy, A.K., 2001. Imaging protein–protein interactions using fluorescence resonance energy transfer microscopy. Methods 24 (3), 289–296.
Loo, Y.M., Melendy, T., 2004. Recruitment of replication protein A by the papillomavirus E1 protein and modulation by single-stranded DNA. J. Virol. 78 (4), 1605–1615.
Masterson, P.J., Stanley, M.A., Lewis, A.P., Romanos, M.A., 1998. A C-terminal helicase domain of the human papillomavirus E1 protein binds E2 and the DNA polymerase alpha-primase p68 subunit. J. Virol. 72 (9), 7407–7419.
Mayer, M.L., Pot, I., Chang, M., Xu, H., Aneliunas, V., Kwok, T., Newitt, R., Aebersold, R., Boone, C., Brown, G.W., Hieter, P., 2004. Identification of protein complexes required for efficient sister chromatid cohesion. Mol. Biol. Cell 15 (4), 1736–1745.
McPhillips, M.G., Oliveira, J.G., Spindler, J.E., Mitra, R., McBride, A.A., 2006. Brd4 is required for E2-mediated transcriptional activation but not genome partitioning of all papillomaviruses. J. Virol. 80 (19), 9530–9543.
McPhillips, M.G., Ozato, K., McBride, A.A., 2005. Interaction of bovine papillomavirus E2 protein with Brd4 stabilizes its association with chromatin. J. Virol. 79 (14), 8920–8932.
Moldovan, G.L., Pfander, B., Jentsch, S., 2006. PCNA controls establishment of sister chromatid cohesion during S phase. Mol. Cell 23 (5), 723–732.
Parish, J.L., Bean, A.M., Park, R.B., Androphy, E.J., 2006a. ChlR1 is required for loading papillomavirus E2 onto mitotic chromosomes and viral genome maintenance. Mol. Cell 24 (6), 867–876.
Parish, J.L., Rosa, J., Wang, X., Lahti, J.M., Doxsey, S.J., Androphy, E.J., 2006b. The DNA helicase ChlR1 is required for sister chromatid cohesion in mammalian cells. J. Cell Sci. 119 (Pt 23), 4857–4865.
Petronczki, M., Chwalla, B., Siomos, M.F., Yokobayashi, S., Helmhart, W., Deutschbauer, A.M., Davis, R.W., Watanabe, Y., Nasmyth, K., 2004. Sister-chromatid cohesion mediated by the alternative RF-CCtf18/Dcc1/Ctf8, the helicase Chl1 and the polymerase-alpha-associated protein Ctf4 is essential for chromatid disjunction during meiosis II. J. Cell Sci. 117 (Pt 16), 3547–3559.
Piston, D.W., Kremers, G.J., 2007. Fluorescent protein FRET: the good, the bad and the ugly. Trends Biochem. Sci. 32 (9), 407–414.
Schweiger, M.R., You, J., Howley, P.M., 2006. Bromodomain protein 4 mediates the papillomavirus E2 transcriptional activation function. J. Virol. 80 (9), 4276–4285.
Senechal, H., Poirier, G.G., Coulombe, B., Laimins, L.A., Archambault, J., 2007. Amino acid substitutions that specifically impair the transcriptional activity of papillomavirus E2 affect binding to the long isoform of Brd4. Virology 358 (1), 10–17.
Skiadopoulos, M.H., McBride, A.A., 1998. Bovine papillomavirus type 1 genomes and the E2 transactivator protein are closely associated with mitotic chromatin. J. Virol. 72 (3), 2079–2088.
Skibbens, R.V., 2004. Chl1p, a DNA helicase-like protein in budding yeast, functions in sister-chromatid cohesion. Genetics 166 (1), 33–42.
Spalholz, B.A., Byrne, J.C., Howley, P.M., 1988. Evidence for cooperativity between E2 binding sites in E2 trans-regulation of bovine papillomavirus type 1. J. Virol. 62 (9), 3143–3150.
Wu, S.Y., Chiang, C.M., 2007. The double bromodomain-containing chromatin adaptor Brd4 and transcriptional regulation. J. Biol. Chem. 282 (18), 13141–13145.
Wu, S.Y., Lee, A.Y., Hou, S.Y., Kemper, J.K., Erdjument-Bromage, H., Tempst, P., Chiang, C.M., 2006. Brd4 links chromatin targeting to HPV transcriptional silencing. Genes Dev. 20 (17), 2383–2396.
You, J., Croyle, J.L., Nishimura, A., Ozato, K., Howley, P.M., 2004. Interaction of the bovine papillomavirus E2 protein with Brd4 tethers the viral DNA to host mitotic chromosomes. Cell 117 (3), 349–360.
zur Hausen, H., 2009. Papillomaviruses in the causation of human cancers—a brief historical account. Virology 384 (2), 260–265.